Available online at www.sciencedirect.com
SCIENCE DIRECT®
Journal of the European Ceramic Society 25 (2005) 1041–1048
www.elsevier.com/locate/jeurceramsoc

Behaviour of the wettability of a SiAlON-base ceramic by molten steel

A. A. Amadeh [a], J. C. Labbe [b], P. E. Quintard [b,c,*]

[a] *Department of Metallurgy and Materials, Faculty of Engineering, Teheran University, P.O. Box 11365-4562, Teheran, Iran*
[b] *Laboratoire de Science des Procédés Céramiques et Traitements de Surface (S.P.C.T.S, UMR 6638 du CNRS), Faculté des Sciences et Techniques, 123 av. Albert Thomas, F-87060 Limoges, France*
[c] *Institut Universitaire de Technologie du Limousin, Allée André Maurois, F-87065 Limoges, France*

Received 9 April 2003; received in revised form 5 February 2004; accepted 25 February 2004
Available online 13 July 2004

Abstract

The purpose of this work is to investigate the wettability and the corrosion of a SiAlON ceramic with amorphous carbon additive (5, 10 and 20 wt.%) by a SiCa treated liquid steel. The carbon additive provokes a change in the substrate nature during the sintering process. Meanwhile these substrates are not wetted and exhibit a relatively good resistance to the corrosion by molten steel mainly because of the formation of a continuous alumina layer on the substrate resulting from SiAlON oxidation. An analysis of the solid–liquid interface allows explaining the corrosion mechanisms.

Keywords: Wetting; Sialons; Steel; Refractories; Corrosion

1. Introduction

Due to the importance and the cost of chemical corrosion of refractory materials and the contamination of steel in metallurgical industry, the interactions between liquid steel and ceramic materials have to be minimised. The β′SiAlON is actually a very studied ceramic material in the industry because of its well known thermomechanical performances at elevated temperatures.[1,2] In steelmaking industry, the carbon additive is commonly used in refractory components in order to improve their thermal shock resistance. It is the reason why we were interested in studying the interaction between a SiAlON–carbon mixture and liquid steel. Our study was based on the wettability and corrosion of sintered ceramic substrates by molten steel. The purpose was to minimise the refractory corrosion via lowering the metal–ceramic contact surface. This can be obtained by reducing the wettability of the solid ceramic by liquid steel. Wetting was studied by the sessile drop method and corrosion through the characterization of the solid–liquid interfaces. The analysis of the solid–liquid interface and the results of wettability allow to explain the corrosion mechanisms.

Although the results are obtained on a few grams in a well controlled atmosphere, this evolution can send back information transferable for a ceramic optimisation in high tonnage ingots or continuous casting.

2. Experimental

2.1. Starting materials

The SiAlON powder was supplied by Pechiney-Electrometallurgy with a granulometry of $d_{50} < 4\,\mu m$. The chemical analysis of this powder is given in Table 1. The X-ray diffraction pattern of this powder shows the presence of small quantities of alumina as impurity.

The amorphous carbon powder “lamp-black” is commercialised by Prolabo and has a granulometry of 0.2–0.3 μm. After burning in oxygen atmosphere the residual ash is less than 0.75%. The steel used is a SiCa treated steel whose melting point is 1515 °C. Its chemical composition is given in Table 2.

2.2. Substrate sintering

Three substrates with 5, 10 and 20% by weight of carbon are prepared by uniaxial pressure sintering in a graphite resistor furnace in a nitrogen atmosphere (1.15×10^5 Pa). The

* Corresponding author.
E-mail addresses: labbe@unilim.fr (J.C. Labbe), quintard@unilim.fr (P.E. Quintard).

0955-2219/$ – see front matter. © 2004 Published by Elsevier Ltd.
doi:10.1016/j.jeurceramsoc.2004.02.020

Table 1
Chemical composition of the used β′SiAlON

	Element (major only)				
	Si	Al	O	N	Ca
Percent	35.4	24.3	20	20	0.3

Table 2
Chemical composition of the used steel (major only)

	Element (major)					
	C	Mn	P	S	Si	Al
Percent	0.0809	1.396	0.016	0.0038	0.344	0.031
	Element					
	B	Ca	N_2	O_2	Fe	
ppm	3	1	32	9	Bal.	

sintering temperature is 1770 °C and a dwelling time of 1 h is performed under a pressure of 25 MPa.[1] These substrates were machined after sintering and then polished with SiC paper during 10 min. The densification rate was 99% for the substrates containing 5 and 10% carbon and 90% for the one with 20% carbon. The surface roughness obtained after polishing is 0.30–0.50 μm for the different percentages of carbon additives. The characterization of the substrates by X-ray diffraction and micro-Raman spectrometry presents an evolution of the substrate structure during sintering. This evolution leads to a decrease of the SiAlON quantity as well as the formation of silicon carbide and aluminium nitride[1,2] in the substrate beside of SiAlON and carbon (Fig. 1).

2.3. Experimental procedure

The contact angle (θ) that characterizes the wettability of a solid substrate by a liquid was measured by the sessile drop method (Fig. 2).

The experimental arrangement allowing the measurement of the contact angle and the solid–liquid tension (σ_{SL}) is given in Fig. 3.

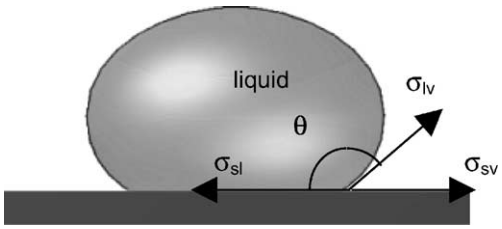

Fig. 2. Sessile drop on an ideal substrate (flat, smooth and horizontal).

The accuracies given hereunder are obtained at a 98% confidence level (Student's t test) from a three times measurement.[3] They are slightly lower than that given in our initial study[4,5] of the precision measurement of our apparatus and its analysis method. The marks on the figure curves indicate the increment of the measurements.

The device consists of a CCD camera (25 images/s) in conjugation with a furnace heated by a graphite resistor. The maximum usable temperature is around 1650 °C. The stability and horizontality of the samples are ensured. The drop and its substrate are observed through quartz windows.

The resistor incandescence is high enough to illuminate the drop at temperatures above 1000 °C. The almost 430,000 (756 × 572) square pixels of the camera sensor and the macro-lens provide a 16 μm resolution. A Matrox™ METEOR frame grabber digitalizes the pictures from the camera.

Wetting experiments were performed in a very pure argon atmosphere (10^{-5} hPa) as a function of temperature up to 1625 °C with a rate of 4 °C/min and also as a function of time at two constant temperatures 1550 and 1570 °C which are usual casting temperatures. After cooling, the drops were cut perpendicularly to the interfaces, polished with SiC paper and 3 μm diamond paste during 10 min and then the characterization by optical microscopy, X-ray diffraction, SEM and micro-Raman spectroscopy were performed.

When hydrostatic pressure is balanced by capillary tension, the mechanical equilibrium everywhere on the liquid surface, can be described by the Laplace's

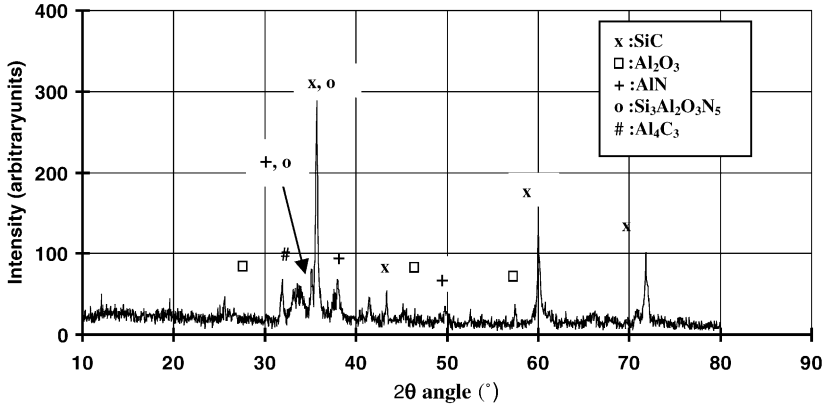

Fig. 1. X-ray diffraction pattern of a 80%SiAlON–20%C sintered substrate.

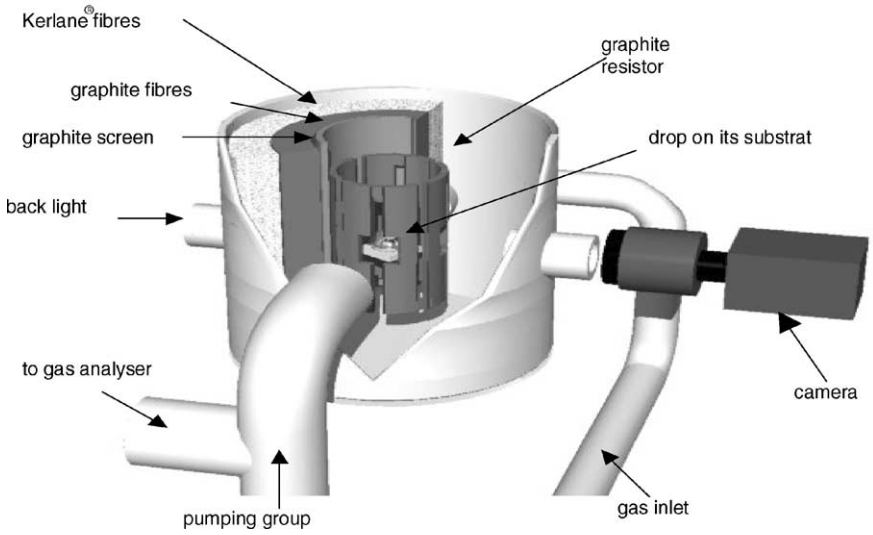

Fig. 3. High temperature sessile drop method experimental set-up.

equation:

$$\sigma_{LV}\left(\frac{1}{R_1}+\frac{1}{R_2}\right)=\rho g z+2\frac{\sigma_{LV}}{b} \quad (1)$$

with σ_{LV}, surface tension of the liquid; R_1, R_2, principal radii of curvature; ρ, density difference between liquid and surrounding fluid, equivalent to liquid density in solid–liquid–gas systems; g, gravitational acceleration; b, radius of curvature at the apex (where $R_1 = R_2$).

Using Bashforth and Adam's notation (Fig. 4),[6] the previous Eq. (1) becomes:

$$\frac{b}{R}+\frac{b}{x}\sin\phi=2+\frac{\beta z}{b} \quad (2)$$

with R, radius of curvature, e.g. R_1 on section P_1; ϕ, angle between (O_2M) and the vertical axis, and $\beta = (\rho g b^2/\sigma_{LV})$, shape factor.

The shape factor β characterizes the difference between the drop profile and a circle.[7,8]

The transformation of profile points from polar co-ordinates to Cartesian co-ordinates provides expressions for R and $\sin\phi$ depending on x and z.

The Laplace Eq. (1) becomes:

$$b\frac{d^2z}{dx^2}+\frac{b}{x}\left(1+\frac{dz}{dx}\right)^2\frac{dz}{dx}=\left(2+\frac{\beta z}{b}\right)\left[1+\left(\frac{dz}{dx}\right)^2\right]^{3/2} \quad (3)$$

The same expression was obtained by Shanahan,[8,9] derived from a minimisation of the free energy in a solid–liquid–gas system. This non-linear second-order differential equation is analytically insoluble. An approximate solution can be obtained either graphically or by numerical integration with a computer. In any case, the generated computed profile of the drop is compared to the experimental one and the difference between the two lines is minimised. This allow to calculate the surface tension σ_{LV} from the

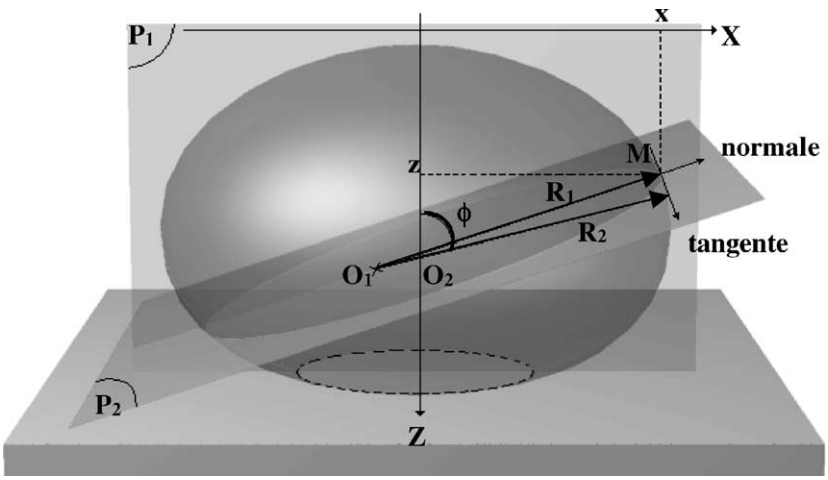

Fig. 4. Representation of Bashforth Adam's equation variables.

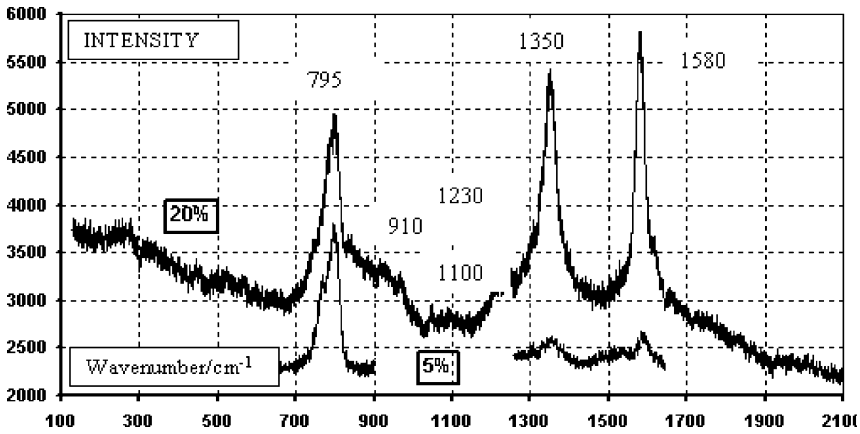

Fig. 5. Micro-Raman spectrum of the sintered substrate, 80%SiAlON–20%C and 95%SiAlON–5%C.

optimal β value; and the contact angle Θ from the slope at $z = 0$ of the calculated profile.

2.4. Micro-Raman experiments

The Raman spectroscopy experiments provide useful informations about the diagnostic of the material and the structure, on the scale of a few lattice constants, amorphous or not. It begins to be used in ceramic/steel analysis. The Raman spectra were obtained at ambient conditions in the range 100–2000 cm^{-1} range using a Dilor spectrometer (XY model) equipped with a charge-coupled device (CCD) detector and an Ar^{+} laser (514.5 nm exciting line), in a backscattering geometry, through a microscope (objective 100×). The area observed is around a few square micron surface on the sample with a penetration depth of ∼0.5 μm. The laser power was chosen up to 100 mW, but after crossing the fore monochromator and after the different losses of energy along the optical pass, the power on the sample was less than 6 mW. Under such conditions the temperature on the sample was inferior to 400 K as checked by the intensity of the Stokes/anti-Stokes bands.

A typical spectrum of a sintered substrate with 5 and 20% carbon is given in Fig. 5. The bands at 1580 and 1350 cm^{-1} are assigned[10] to amorphous carbon. The wide band centred at nearly 910 cm^{-1} is assigned to the vibrations of the bridge Si–O–Si and Si–O–Al and the band at 796 cm^{-1} is characteristic of SiC.[11,12] The broad band at 1100 cm^{-1} evidences alumina.

AlN when present shows an intense band at 660 cm^{-1} with a shoulder at 610 and a broad band centred at 900 cm^{-1}.

3. Results

3.1. Wetting

3.1.1. Contact angle

The contact angle (θ) of the liquid steel over the substrates containing 10 and 20% of carbon is non-wetting ($\theta >$ 120°) and remains practically constant as a function of temperature. For 5% of carbon additive it decreases at 1560 °C and then remains nearly constant above 1570 °C. It must be noted that in this case a solid layer appears at the surface of the drop just after melting and disappears at 1560 °C when the contact angle starts to decrease (Fig. 6).

The time dependent experiments at 1550 and 1570 °C during 1 h also show the non-wetting contact angles higher than 120° for all of the substrates.

3.1.2. Liquid–vapour tension

The liquid–vapour tension (σ_{LV}) remains nearly constant (accuracy ± 2%) for the substrate with 0 and 5% of carbon. It decreases continuously after a small increase in the other cases. The high values of this parameter in the later cases must be attributed to the drop swelling observed notably until 1550 °C and/or to the formation of a solid layer at the drop surface (Fig. 7).

3.1.3. Solid–liquid tension

The solid–liquid interfacial tension (σ_{SL}) was calculated using the Young's equation: $\sigma_{SL} = \sigma_{SV} - \sigma_{LV}\cos\theta$.

The solid–vapour tension (σ_{SV}) used in this equation is unknown for the SiAlON–carbon mixtures, but because our main interest lies in the evolution of σ_{SL} more than in its absolute values, we consider in our calculation a constant value for solid–vapour tension equal to 1000 mN/m as it was previously proposed[13–16]. In such a way the σ_{SL} evolution as a function of time, given in Fig. 8, passes through a minimum for the substrate containing 5% of carbon. According to several authors[17] this kind of evolution is a proof of a chemical interaction at the solid–liquid interface. For the other substrates σ_{SL} decreases slightly.

3.1.4. Work of adhesion

The work of adhesion was computed by using the equation $W_{ad} = \sigma_{LV}(1 + \cos\theta)$. Its evolution, illustrated in Fig. 9 for different temperatures, shows an increase with temperature rising for the substrate containing 5% of carbon. For the 10

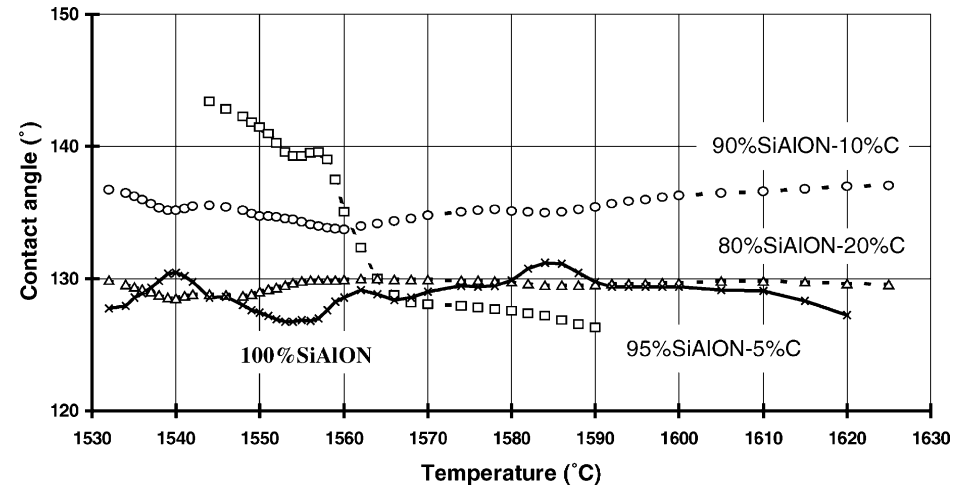

Fig. 6. Evolution of the contact angle vs. temperature (accuracy ± 1%).

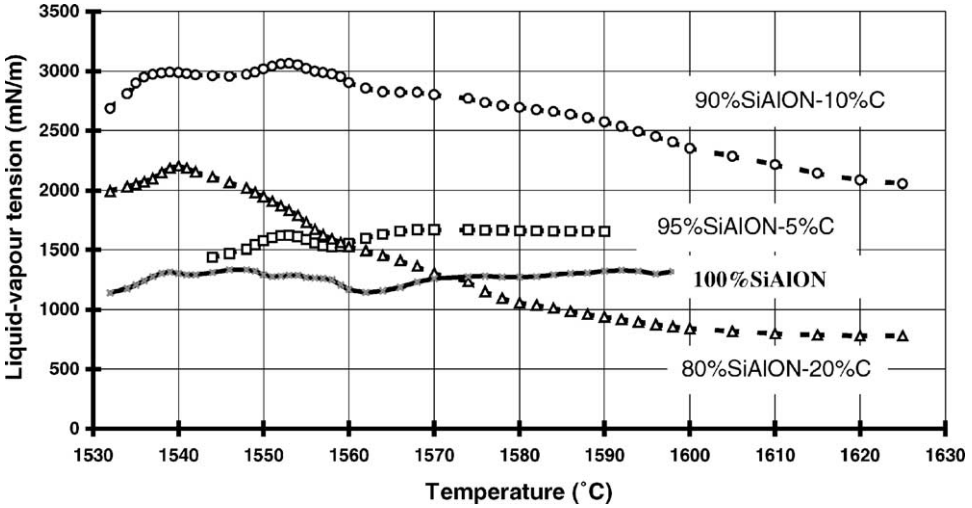

Fig. 7. Evolution of the liquid–vapour tension with temperature (accuracy ± 2%).

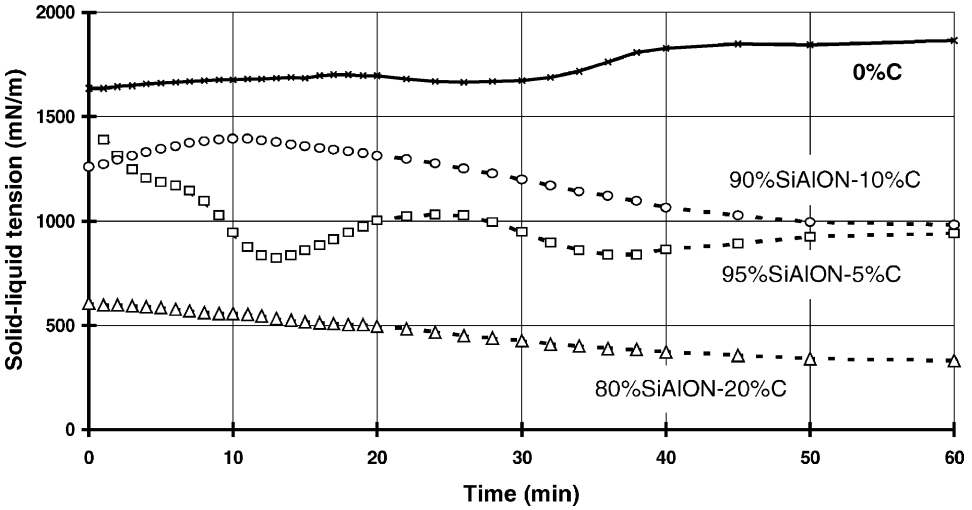

Fig. 8. Evolution of the solid–liquid tension vs. time at 1570 °C (accuracy ± 2%).

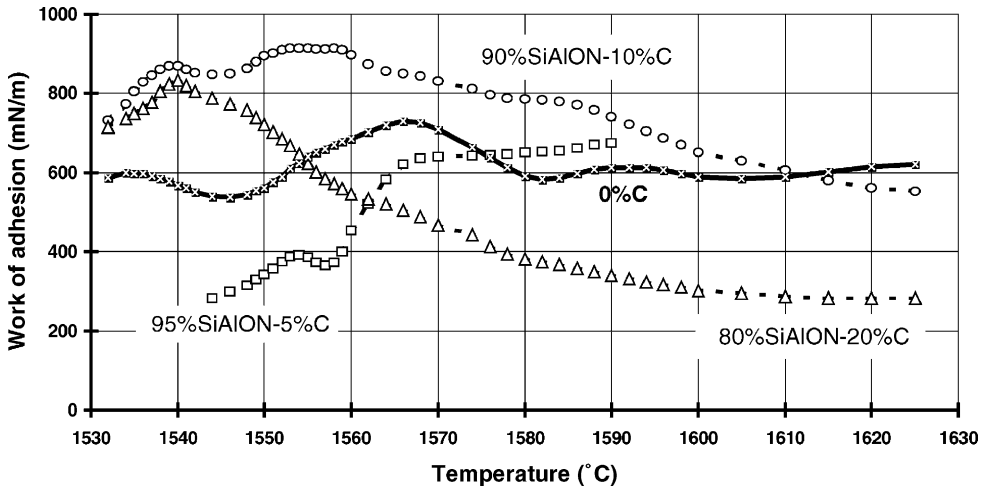

Fig. 9. Evolution of the work of adhesion with temperature (accuracy ± 5%).

and 20% additives it decreases continuously at temperatures above 1560 and 1540 °C, respectively.

In Fig. 10 we give the evolution of the work of adhesion versus carbon content for two usual casting temperatures. It was measured after a 60 min dwell time. The work of adhesion is low (<1000 mN/m) and is reduced by increasing carbon content except for the 5% carbon additive which on the other figures also exhibit anomalies which are discussed.

3.2. Chemical composition of molten steel

During the experimentations we remarked that the melting point of the steel decreases and the first liquid at the metal–ceramic interface appears at a temperatures lower than the melting point of our steel (at 1400 °C over the substrate containing 20% of carbon instead of 1515 °C). This leads us to analyse the molten steel after contact with ceramic substrate. A typical analysis performed on a steel drop after 1 h of contact with the 80%SiAlON–20%C substrate at 1570 °C is presented in Fig. 11. It shows an enrichment in carbon, aluminium and silicon content of the steel.

3.3. Interface characterization

The observation of the solid–liquid interfaces by SEM discloses that the substrate containing 20% carbon was greatly corroded by the molten steel. The iron has penetrated over a thickness of 70 μm in the substrate. In contrast, the corrosion thickness over the other substrates was not detected.

The X-ray diffraction pattern of these substrates, out of the contact zone with liquid steel, exhibits Al_2O_3 phase and an increase in AlN pics relative intensity (Fig. 12).

Indeed, the micro-Raman spectrum of the substrates with 5 and 10% of carbon, illustrated in Fig. 13, does not show the amorphous carbon pics that will appear at 1350 and 1580 cm^{-1} [10] (see Fig. 2).

In addition, over the same substrates in the contact zone with liquid steel, a white phase appears which presents the characteristic micro-Raman bands of AlN[18,19] and alumina (more clear on the X-ray spectrum). This substrate, after interaction with the liquid steel, no longer presents Raman carbon bands.

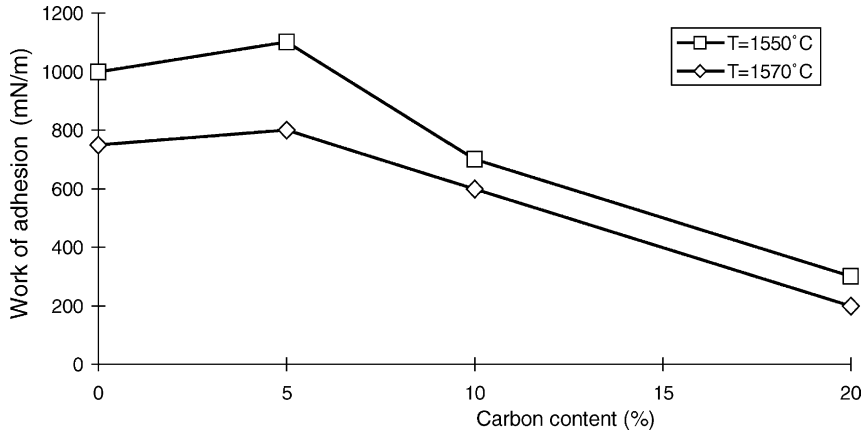

Fig. 10. Evolution of the work of adhesion with carbon content at two usual casting temperatures after a dwell time of 60 min.

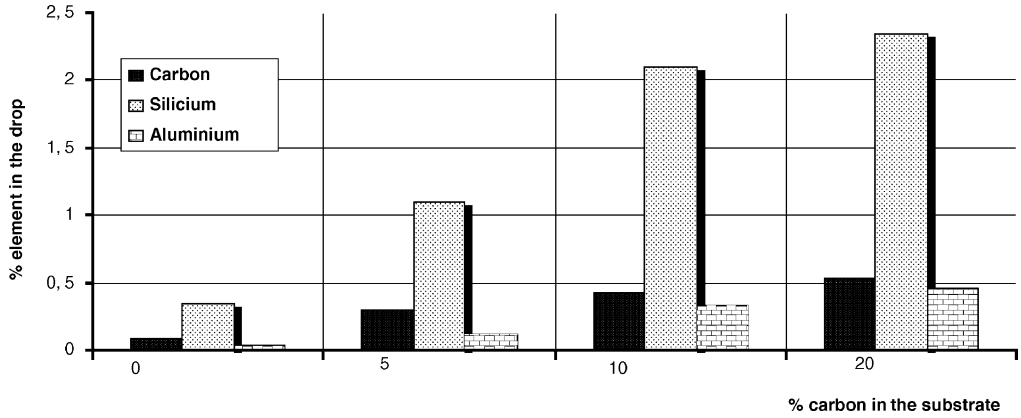

Fig. 11. Chemical analysis of the steel drop after 1 h contact with a substrate. For 0, 5, 10 and 20% carbon content.

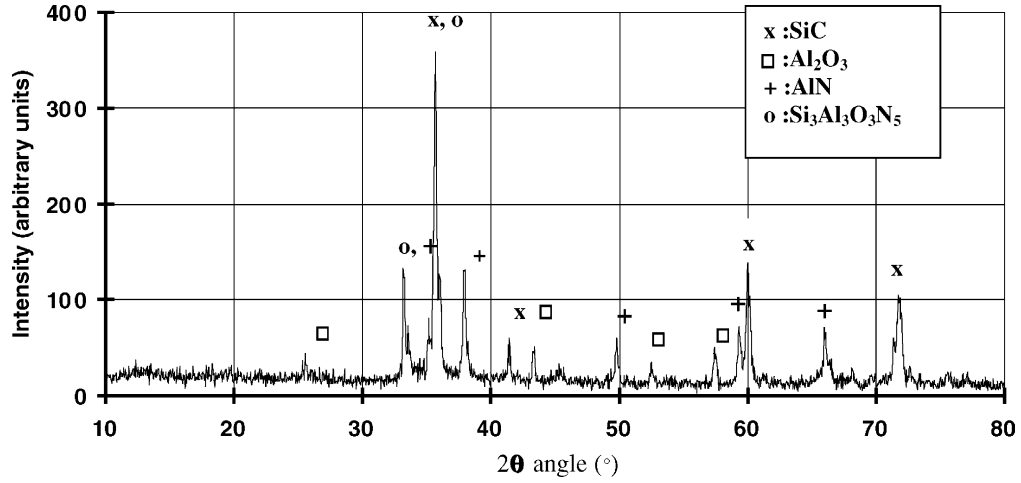

Fig. 12. X-ray diffraction pattern of a 80%SiAlON–20%C after experimentation.

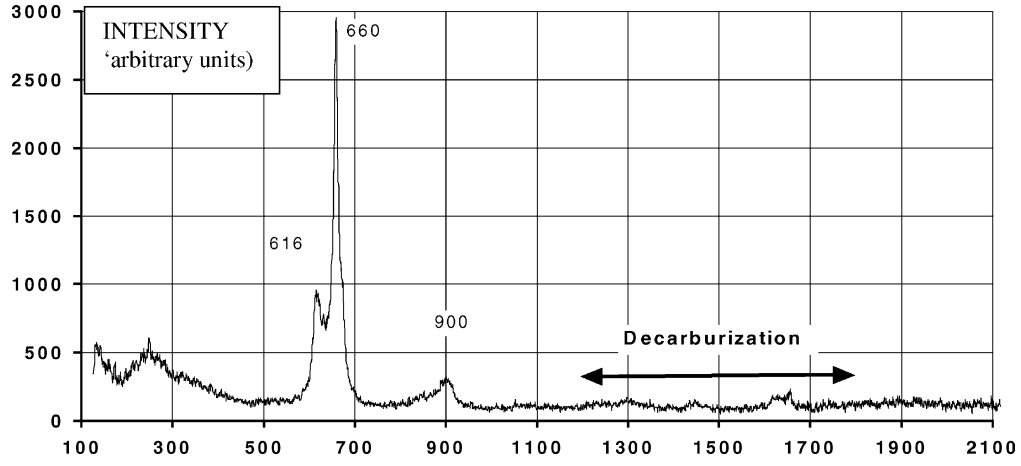

Fig. 13. Micro-Raman spectrum of a 90%SiAlON–10%C substrate after experimentation.

4. Discussion

These results and observations allow to conclude that during the experimentation the substrate is the seat of a complex transformation checked by

- a decrease in the intensity of X-ray SiAlON pics;
- the formation of aluminium nitride and alumina;
- the vanishing of carbon in the superficial layers in contact with the liquid steel of the substrates containing 5 and 10% of carbon; and

- a correlative enrichment of the steel in carbon, aluminium and silicon.

Consequently, the substrate corrosion must be explained through a SiAlON decomposition in AlN, Si and volatile species such as Al_2O, AlO and AlO_2, followed by an AlN decomposition in Al and N_2. The carbon added in the substrate and the Si dissolves in the steel liquid phase. The SiAlON becomes oxidized with residual oxygen (20 ppm) in our furnace whose result will be the formation of an Al_2O_3 layer[20,21] according to the reactions:

$\beta'\text{SiAlON} \rightarrow \text{SiAlON15R}$ followed by

$\text{SiAlON15R} \rightarrow Al_2O_3$

Our previous studies[22,23] have shown that pure AlN is wetted and greatly corroded while pure alumina is not wetted nor corroded by this kind of liquid steel. Thus, we can conclude that the presence of this high purity alumina layer can protect the substrate against the corrosion by liquid steel.

The decrease in steel melting point observed during the experimentation must be assigned on one hand to the dissolution of the carbon present in the substrate and on the other hand to thermal dissociation of SiC, followed by the dissolution of the resulting elements in the liquid phase.[24] At 1673 K:

$$C_{(\text{substrate})} \rightarrow [C]_{\text{steel}}, \quad \Delta G^\circ = -48.11\,\text{kJ/mol}$$

$$SiC_{(\text{substrate})} \rightarrow [Si]_{\text{steel}} + [C]_{\text{steel}}, \quad \Delta G^\circ = -143.92\,\text{kJ/mol}$$

The dissolution of carbon and silicon decreases the steel melting point according to the iron–carbon[25] and iron–silicon[26] binary diagrams.

Finally, the addition of 10–15% carbon in the sialon matrix leads to an increase in the contact angle, and a correlative decrease of the wettability, and of the work of adhesion with a lowering of the interaction with steel during the casting process.

5. Conclusions

The carbon additive in SiAlON ceramics leads to a change of substrate nature during the sintering process to a mixture of SiAlON–C–SiC–AlN. During the wetting experimentation, the SiAlON decomposition is going on. The SiAlON base substrates are not wetted by the SiCa treated liquid steel. These substrates present a relatively good resistance against the corrosion by molten steel. This resistance can be in part imputed to the in situ formation of a high purity and continuous layer of alumina resulting from the SiAlON oxidation.

The decrease of the wettability and the work of adhesion with 10–15% addition of carbon leads to minimise the interaction between the sialon matrix and the liquid steel during the continuous casting process, this can explain the observed lowering of contamination.

References

1. Brossard, M., *Solution Solid SiAlON β′*. Ph.D. thesis, University of Limoges, No. 14, 1986.
2. Desmaison, J. and Riley, F. L., The oxidation of SiAlON materials. *J. Mater. Sci.* 1981, **16**, 2625–2628.
3. Mandel, J., *The Statistical Analysis of Experimental Data*. Dover, New York, 1984.
4. Labbe, J. C., Lachau-Durand, A. *et al.*, Utilisation de l'analyse d'image dans la determination de la tension superficielle d'une goutte de metal fondu. *High Temp. Chem. Process.* 1992, **1**, 151–156.
5. Leroux, V., Labbe, J. C., Shanahan, M. E. R. *et al.*, Contact angle and surface tension measurements on a metal drop by image processing and numerical calculation. *High Temp. Chem. Process.* 2000, **4**, 351–364.
6. Bashforth, F. and Adams, S. C., *An Attempt to Test the Theories of Capillarity*. Cambridge University Press, 1883.
7. Praday, J. F., *Surface Tension II, Surface and Colloid Science*, *Vol 1*, ed. E. Matijevic. Wiley Interscience, New York, 1969.
8. Shanahan, M. E. R., *Adhesion, Vol 6*, ed. K. M. Allen. Applied Science Publishers, 1982, pp. 75–82.
9. Shanahan, M. E. R., *J. Chem. Soc. Faraday Trans. I* 1982, **78**, 2701–2710.
10. Huong, P. V., *Diamond Relat. Mater.* 1991, **1**, 33–41.
11. Nakamoto, K., *Infrared and Raman Spectra of Inorganic and Coordination Compounds*. Wiley, New York, 1986.
12. Turrell, G., *Infrared and Raman Spectra of Crystals*. Academic Press, London, 1972.
13. Marija, T. and Kolar, D., *J. Am. Ceram. Soc.* 1978, **61**, 5.
14. Sangiriogi, R., Muolo, M. L. and Passerone, A., *Mater. Sci. Monogr.*, 1987, **38A**(High Tech. Ceram., Part A), 415.
15. Amadeh, A. A., Labbe, J. C., Laïmech, A. and Quintard, P. E., Influence of boron nitride and carbon additives on the behaviour of sintered AlN in a steel-making environment. *J. Eur. Ceram. Soc.* 1996, **16**, 403–408.
16. Amadeh, A. A., Labbe, J. C. and Quintard, P. E., Wettability of AlN–BN–C ceramics by a SiCa treated liquid steel. *Corrosion Sci.* 2004, **46**, 183–191.
17. Aksay, I. A., Hoge, C. E. and Pask, J., *J. Phys. Chem.* 1974, **78**(12), 1178–1183.
18. McNeil, L. E., Grimsditch, M. and French, R. H., Vibrational spectroscopy of aluminium nitride. *J. Am. Ceram. Soc.* 1993, **76**(5), 1132–1136.
19. Brafman, O., Lendyel, G., Mitra, S. S., Gielisse, P. J., Plendl, J. N. and Mansur, L. C., Raman spectra of AlN, BN and BP. *Solid State Commun.* 1968, **6**, 523–526.
20. Brossard, M., Brachet, D., Goursat, P. and Billy, M., *C. R. Acad. Sci. Paris* 1978, **286**, 345–348.
21. Brossard, M., Brachet, D., Goursat, P. and Billy, M., *Ann. Chim. Fr.* 1979, **4**, 7–14.
22. Laïmeche, A., *Contribution à l'etude du comportement des materiaux ceramiques en milieu siderurgique*. Ph.D. thesis, University of Limoges, No. 53, 1993.
23. Labbe, J. C. and Laïmech, A., Study of the behaviour of aluminium nitride in the iron and steel industry. *J. Eur. Ceram. Soc.* 1996, **16**, 893–908.
24. Kalogeropoulou, S., Baud, L. and Eustathopoulos, N., *Acta Metall. Mater.* 1995, **43**(3), 907–912.
25. Anderson, J. C., Leaver, K. D., Rawlings, R. D. and Alexandre, J. M., *Materials Science* (*3rd ed.*). Van Nostrand, UK, 1985.
26. Massalski, T. B., *Binary Alloy Phase Diagrams* (*2nd ed.*). ASM Int., Metals Park, OH, 1990.